Available online at www.sciencedirect.com
SCIENCE DIRECT®
ELSEVIER
Materials Science in Semiconductor Processing 9 (2006) 102–106
MATERIALS SCIENCE IN SEMICONDUCTOR PROCESSING

Photoluminescence analysis of intra-grain defects in cast-grown polycrystalline silicon wafers

H. Sugimoto[a,*], M. Tajima[a], T. Eguchi[b], I. Yamaga[b], T. Saitoh[c]

[a]*Institute of Space and Astronautical Science, Japan Aerospace Exploration Agency, 3-1-1 Yoshinodai, Sagamihara 229-8510, Japan*
[b]*Dai-ichi Dentsu Co., 1-54-1, Shimoishihara, Chofu, Tokyo 182-0034, Japan*
[c]*Tokyo University of Agriculture & Technology, 2-24-16, Naka-cho, Koganei, Tokyo 184-8588, Japan*

Available online 13 February 2006

Abstract

Effects of intra-grain defects in cast polycrystalline silicon (poly-Si) wafers on the solar cell performance were investigated by photoluminiscence (PL) spectroscopy and mapping at room temperature. We confirmed that the crystallinity of the longer diffusion length region of the poly-Si is almost the same as that of the single crystalline Si. For the PL macroscopic mapping, low PL intensity regions correspond to short diffusion length regions. In short diffusion length regions, plenty of dark lines and spots were observed by PL microscopic mapping, while, in contrast, longer diffusion length regions have few of them. These findings showed clearly that dark lines and spots of the PL mapping relate to defects degrading the cell performance. We also found that structures of defects depend on the fabrication process.

Keyword: Photoluminescence; Intra-grain defects; Polycrystalline Si; Solar cell

1. Introduction

Photovoltaic industry is growing extensively and cast-grown polycrystalline silicon (poly-Si) has become a dominant material of solar cells because of the cost-effectiveness. So far, the restraint of mischief of grain boundaries was a key work for fabricating higher-efficiency solar cells. The conversion efficiency of poly-Si cells has been improved by increasing the grain size and using the hydrogen passivation [1,2]. Defects and impurities in a grain also determine cell performances. Recently, effects of intra-grain defects on the conversion efficiency have become larger than those of grain boundaries. Therefore, understanding the electrical activity of such defects is essential to develop high quality poly-Si cells.

Electrical properties of grain boundaries have been minutely investigated by the electron-beam-induced current (EBIC) technique [3], however, there are a few reports on intra-grain defects of the poly-Si [4]. The purpose of this work was to investigate intra-grain defects, which degrade cell performances. Photoluminescence (PL) spectroscopy is known to be one of the most sensitive techniques for characterizing defects and impurities in semiconductors. In this study, we applied the PL technique to characterize defects in cast poly-Si wafers.

*Corresponding author. Tel./fax: +81 42 759 8329.
E-mail address: sugimoto@isas.jaxa.jp (H. Sugimoto).

1369-8001/$ - see front matter
doi:10.1016/j.mssp.2006.01.033

2. Experimental technique

2.1. Samples

Cast poly-Si ingots fabricated by the unidirectional solidification technique were sliced vertically into thin wafers. We prepared two types of wafers. Samples A and B were fabricated with the rapid and slow solidification, respectively. Sample B had extremely large grain size, which exceeded a few centimeters. They were boron doped ($1 \times 10^{16}\,cm^{-3}$) with a resistivity ranging from 1.0 to 1.5 Ω cm, a thickness of 2.8 mm and the size of $180 \times 130\,mm^2$. To remove sowing damages, they were etched off by the HNO_3/HF solution. Measurements of the minority carrier diffusion length and the PL were performed on as grown wafers. Distributions of the minority carrier diffusion length were examined by the surface photovoltage (SPV) technique. The average diffusion length of the electron was 400 μm (sample A) and 360 μm (sample B), respectively.

2.2. Experimental conditions

PL spectroscopy was performed at room temperature. Samples were excited by the 532 nm line of a ND:YVO_4 laser, which had the penetration depth of about 1.4 μm to Si. The excitation power and laser beam diameter were 30 mW and 2.0 mm, respectively. PL from samples was transferred to a monochromator (Jobin Yvon HR320, $f = 320$ mm, $F = 4.2$) with 600 groove/mm grating blazed at 1.0 μm and detected by a Ge pin diode (North Coast EO-817L) cooled at 77 K. The detected signal was processed with a lock-in technique and then transferred to a computer for various data processing. The spectral response of the measurement system was calibrated with blackbody radiation.

PL macroscopic and microscopic mappings were performed at room temperature using a unique mapping system, which had an accurate and fast X–Y stage with position-repeatability as high as ±0.3 μm and with a maximum translation speed of 100 mm/s [5]. The spatial resolution of the macroscopic and microscopic mappings, which was determined by the beam diameter, was about 300 and 10 μm, and the excitation power was about 10 and 0.1 mW, respectively. These excitation powers and beam diameters were selected for the optimum measurement. Luminescence light was collected by the objective, passed through the band-pass filters with the transmission band of 1050–1230 nm, and detected by a photomultiplier (Hamamatsu R5509-72). The detected signal was processed with the lock-in technique. The interval of the sampling points for macroscopic and microscopic mapping was 500 and 1 μm, respectively. A typical time required for a full wafer mapping was about 30 min.

3. Results and discussion

3.1. PL spectroscopy

Near band-edge, PL spectra from the shorter and the longer minority carrier diffusion length region on samples A and B were obtained by the PL spectroscopy at room temperature. We show PL spectra of the longer diffusion length region on samples A, B and a typical single crystalline Si (SC-Si) in Fig. 1. The PL intensity of sample A is 20% higher than that of sample B. That of SC-Si is higher than that of poly-Si. However, the full-width at half-maximum (FWHM) of PL spectra are hardly different. This shows that the crystallinity of the longer diffusion length region on samples A and B are almost the same as that of SC-Si.

PL intensity of the shorter diffusion length region is less than 20% that of the longer diffusion length region, and the FWHM of PL spectrum of the former region is 18% wider than that of the latter region. Deep-level emission is below our detection limit. From these results, we confirmed that the crystallinity of the shorter diffusion length region is degraded.

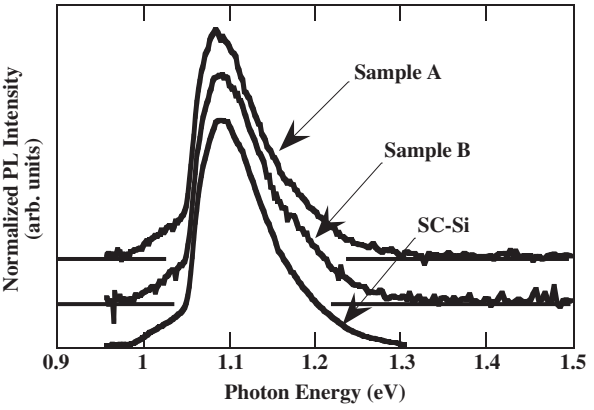

Fig. 1. PL spectra from sample A, sample B and typical single crystalline Si (SC-Si) wafer at room temperature. Each PL intensity was normalized.

3.2. PL macroscopic mapping

Comparison between the distribution of minority carrier diffusion length and the PL macroscopic mapping on sample A is shown in Fig. 2. Low PL intensity regions were observed on the periphery and the upper center regions of the sample. We found that these regions correspond to the short diffusion length regions. The degradation of the diffusion length on the periphery is known to be due to the iron contamination during the solidification of the ingot. So far, the reason for the degradation of the diffusion length on the upper center regions has not been solved yet. The high spatial resolution of the PL mapping enables us to find that dark patterns exist in these regions. We confirmed that these dark patterns are not due to surface scratches, because the same patterns were obtained from backside of the sample.

High PL intensity regions do not correspond to the long diffusion length regions; the PL intensity increases on upper regions of the sample while the long diffusion length regions exist on the center. We can estimate this is because upper regions of the sample have a low resistivity, that is, a high impurity concentration.

Comparison between the distribution of minority carrier diffusion length and the PL macroscopic mapping on sample B is shown in Fig. 3. Just same

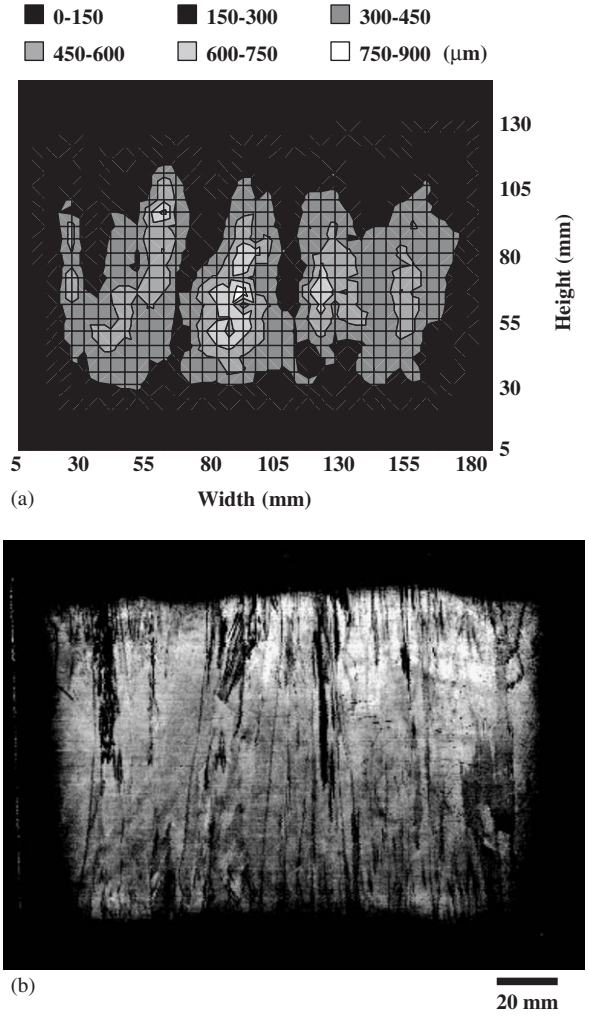

Fig. 2. Comparison between (a) distribution of minority carrier diffusion length and (b) PL macroscopic mapping ($185 \times 140\,cm^2$) on sample A. Whiter regions indicate higher PL intensity. Interval of sampling points is about (a) 5 mm and (b) 0.5 mm, respectively.

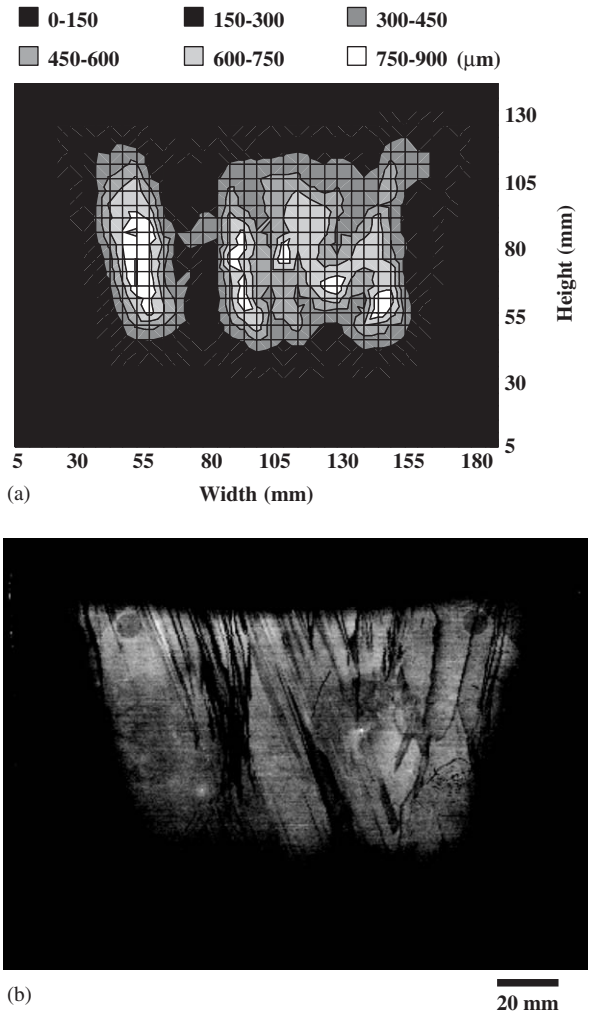

Fig. 3. Comparison between (a) distribution of minority carrier diffusion length and (b) PL macroscopic mapping ($185 \times 140\,cm^2$) on sample B. Interval of sampling points is (a) 5 mm and (b) 0.5 mm, respectively.

as sample A, low PL intensity regions were observed on the periphery and the upper center regions of the sample. We also confirmed that low PL intensity regions correspond to the short diffusion length regions. Dark areas on the periphery spread wider than that of sample A. This is because sample B was suffered from plenty of the iron contamination during the long-term solidification. In the PL mapping, we can find that dark lines exist on center regions. High PL intensity regions do not correspond to the long diffusion length regions; this is also due to the fact that upper regions of the sample have a low resistivity.

From these results, we estimated that these dark lines relate to the very defects which degrade the cell performances.

3.3. PL microscopic mapping

We zoomed into the short and long diffusion length regions on samples A and B with the PL microscopic mapping, as shown in Figs. 4 and 5. Fig. 4(a) shows the short diffusion length region of sample A. There are plenty of dark lines and some dark planes; densities of these patterns are about 2000 lines/cm^2 and 30 planes/cm^2. Since contrasts of the background indicates grain boundary, we found these dark patterns are not grain boundary. The long diffusion length region of sample A is shown in Fig. 4(b). There are few lines; the density of dark lines (about 20 lines/cm^2) is much less than that of short diffusion length regions.

We investigated more closely around characteristic micro-patterns of sample A, as illustrated in Fig. 4(1)–(4). We found that many kinds of micro-patterns exist, such as (1) twin lines, (2) twin curved lines, (3) a lope and (4) spirals.

Fig. 5(a) presents the short diffusion length region of sample B. Patterns are quite different from sample A; almost all patterns are dark planes (about 100 planes/cm^2). The long diffusion length region of sample B is shown in Fig. 4(b). Though some dark spirals happen to exist in this region, there are few patterns around over 1 cm^2; the density of patterns is about 5 spilals/cm^2.

We investigated more closely around characteristic micro patterns of sample B, as illustrated in Fig. 5(1)–(4). We also found that many kinds of micro patterns exist, such as (1), (2) planes, (3) spirals and (4) a dot.

In summary, the density of micro-dark patterns of the long diffusion length region is much less than

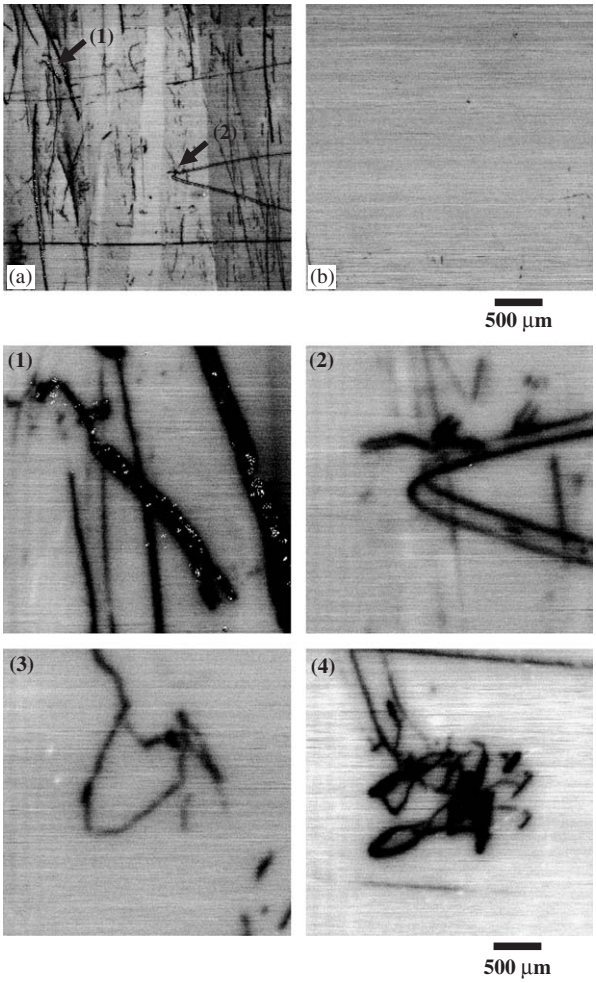

Fig. 4. PL microscopic mappings ($3 \times 3\,mm^2$) in (a) short minority carrier diffusion length region (shorter than 100 μm) and (b) long minority carrier diffusion length region (longer than 700 μm) on sample A. (1)–(4) are PL microscopic mappings ($300 \times 300\,\mu m^2$) nearby characteristic micro-patterns. (1) and (2) are indicated in (a). (3) and (4) were obtained from different areas. Interval of sampling points of (a) and (b) is 10 μm and that of (1)–(4) is 1 μm.

that of the short diffusion length region. We confirmed dark patterns are not grain boundaries. These findings support our conclusion that dark patterns relate to the defects degrading the cell performance.

We observed various dark patterns and found their structures depend on the fabrication process of wafers; dark lines are dominant for the rapid solidification, and dark planes are dominant for the slow solidification.

As a next step, we have to solve what the dark patterns are. Though we consider them dislocations

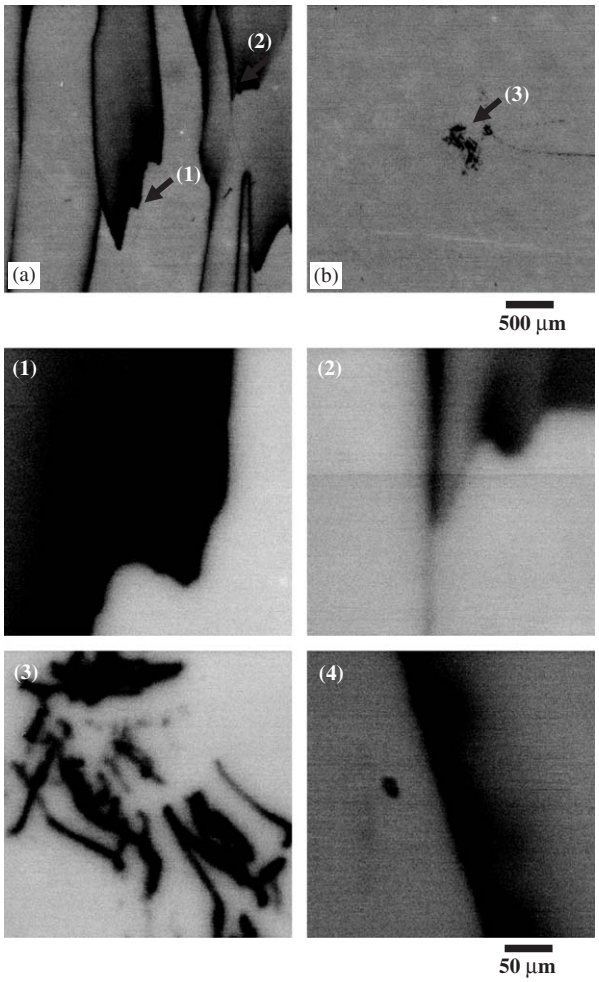

Fig. 5. PL microscopic mappings ($3 \times 3\,mm^2$) in (a) short minority carrier diffusion length region (shorter than 100 μm) and (b) long minority carrier diffusion length region (longer than 700 μm) on sample B. (1)–(4) are PL microscopic mappings ($300 \times 300\,\mu m^2$) nearby characteristic micro-patterns. (1)–(3) are indicated in (a) or (b). (4) was obtained from different area. Interval of sampling points of (a) and (b) is 10 μm and that of (1)–(4) is 1 μm.

contaminated by heavy metals from tentative experiments, more work needs to be done.

4. Conclusions

We investigated intra-grain defects in cast poly-Si wafers by PL spectroscopy and macroscopic and microscopic mapping at room temperature. FWHM of PL spectra from poly-Si samples and the SC-Si are hardly different, which indicates that the crystallinity of the longer diffusion length region of poly-Si is almost the same as that of SC-Si. For the PL macroscopic mapping, low PL intensity regions correspond to short diffusion length regions. In short diffusion length regions, there are many dark patterns of PL microscopic mapping, while; in contrast, the longer diffusion length region has few of them. These findings showed clearly that the dark patterns relate to the defects degrading the cell performance. We also found that structures of dark patterns depend on the fabrication process; dark lines are dominant for the rapid solidification and dark planes are dominant for the slow solidification. Present results allow us to propose that PL mapping has great potential for clarifying the correlation between defects and cell performance.

Acknowledgement

The authors would like to thank Dr. M. Dhamrin for the measurement of the distributions of minority carrier diffusion length. They also thank Prof. Y. Ohshita, Prof. A. Ogura and Prof. K. Kakimoto for contributing useful discussions.

References

[1] Lu J, Wagener M, Rozgonyi G, Rand J, Jonczyk R. Effects of grain boundary on impurity gettering and oxygen precipitation in polycrystalline sheet silicon. J Appl Phys 2003;94(1):140–4.

[2] Carnel L, Gordon I, Nieuwenhuysen KV, Gestel DV, Beaucarne G, Poortmans J. Defect passivation in chemical vapour deposited fine-grained polycrystalline silicon by plasma hydrogenation. Thin Solid Films 2005;487(1,2):147–51.

[3] Chen J, Sekiguchi T, Xie R, Ahmet P, Chikyo T, Yang D, et al. Electron-beam-induced current study of small-angle grain boundaries in multicrystalline silicon. Scr Mater 2005;52(12):1211–5.

[4] Ohshita Y, Nishikawa Y, Tachibana M, Tuong VK, Sasaki T, Kojima N, et al. Effects of defects and impurities on minority carrier lifetime in cast-grown polycrystalline silicon. J Cryst Growth 2005;275(1,2):e491–4.

[5] Tajima M, Li Z, Shimidzu R. Photoluminescence mapping system applicable to 300 mm silicon-on-insulator wafers. Jpn J Appl Phys 2002;41(12b):L1505–7.